# Solution $^1$H NMR Characterization of Axial Interactions of the Proximal and Distal His in the Cyanomet Complexes of the Isolated Chains and the 65 kDa Intact Tetramer of Human Hemoglobin A

**Gerd N. La Mar,* Urszula Kolczak, Anh-Tuyet T. Tran, and Ellen Y. T. Chien**

*Contribution from the Department of Chemistry, University of California, Davis, California 95616*

*Received December 4, 2000. Revised Manuscript Received February 26, 2001*

**Abstract:** Solution $^1$H NMR has been used to investigate the axial bonding of the proximal His and the hydrogen-bonding of the distal His to the bound ligand in the isolated chains as well as the subunits of intact, tetrameric, cyanomet human hemoglobin A. The complete proximal His, including all ring protons necessary to monitor bonding in each subunit, could be definitively assigned by 1D/2D methods despite the large size (∼65 kDa) and severe relaxation (to $T_1 \approx 3$ ms, line width ≈ 1.5 kHz) of two of the protons. The complete distal His E7 ring was assigned in the α-chain and α-subunit of HbA, and the dipolar shifts and relaxation were analyzed to reveal a disposition intermediate between the positions adopted in HbCO and $HbO_2$ that is optimal for forming a hydrogen bond with bound cyanide. The lability of the α-subunit His E7 $N_\epsilon H$ is found to be similar to that in sperm whale cyanomet myoglobin. The orientation of the distal His E7 in the β-subunit is found to be consistent with that seen in either HbCO or $HbO_2$. While the His E7 labile $N_\epsilon H$ proton signal could not be detected in either the β-chain or subunit, it is concluded that this more likely reflects increased lability over that of the α-subunit, and not the absence of a hydrogen bond to the bound ligand. Analysis of the heme mean methyl hyperfine shift, which has been shown to be very sensitive to the presence of distal hydrogen bonds to bound cyanide (Nguyen, B. D.; Xia, Z.; Cutruzzolá, F.; Travaglini Allocatelli, C.; Brancaccio, A.; Brunori, M.; La Mar, G. N. *J. Biol. Chem.* **2000**, *275*, 742−751), directly supports the presence of a distal His E7 hydrogen bond to cyanide in the β-chain and β-subunit which is weaker than the same hydrogen bond in the α-subunit. The potential for the proximal His hyperfine shifts in serving as indicators of axial strain in the allosteric transition of HbA is discussed.

## Introduction

Mammalian hemoglobin, Hb,[1] is composed of tetramers of two nonequivalent ∼150 residue chains, $\alpha_2\beta_2$, with each chain exhibiting the highly conserved fold of 7−8 helices (A−H) with the heme wedged between helices E and F, as found in the monomeric myoglobins.[2,3] The role of Hb is to efficiently bind $O_2$ in the lungs and deposit it in the muscle where it is utilized or stored by Mb. The efficiency of the process is due to the allosteric nature of Hb, where the tetramer can exist in two quaternary or "affinity" states, the T (tense) low-affinity, and R (relaxed) high-affinity states,[4−6] the latter of which has an affinity resembling monomeric Mb. The relative stabilities of the T- and R-states are modulated by protons (Bohr effect), partial ligation (cooperativity), and binding of organophosphate, $CO_2$, or chloride ion binding at sites remote from the heme.[2−5] The properties of the T-state, which differs from the R-state by a 15° rotation of one $\alpha\beta$ dimer relative to the other, is to reduce the affinity by $\sim 10^3$ compared to the R-state, Hb, the separated chains, or Mbs.

Two His, the completely conserved axial His F8, and the highly conserved[2,3,7] (except in opossum Hb)[8] distal His E7 in mammalian Hbs, play focal roles in providing the exquisite control of $O_2$ binding. On one hand, the strong preference for $O_2$ over CO in globins in general, when compared to that in heme outside the protein, is exerted by the distal His E7 by providing a strongly stabilizing hydrogen bond[3−6,9,10] to bound $O_2$. Otherwise, the naturally higher affinity for CO would lead to inhibition of function by CO produced by heme catabolism.[11,12] The crystal structure of $HbO_2$, however, finds that only in the α-subunit is HisE7 ideally oriented to hydrogen bond to the ligand.[9] A weaker or completely absent hydrogen bond to bound $O_2$ in the β-subunit has been inferred from the less than

* Address correspondence to: Dr. Gerd N. La Mar, Department of Chemistry, University of California, Davis, CA 95616. Telephone: (530) 752-0958. Fax: (530) 752-8995. E-mail: lamar@indigo.ucdavis.edu.

(1) Abbreviations used, metHbCN, cyanomet HbA.; met-α-CN, cyanomet α-chain of HbA; met-β-CN, cyanomet β-chain of HbA; metMbCN, cyanomet myoglobin; NOE, nuclear Overhauser effect; NOESY, two-dimensional nuclear Overhauser spectroscopy; TOCSY, two-dimensional total correlation spectroscopy; WEFT, water-eliminated Fourier transform; WT, wild type.

(2) Antonini, E.; Brunori, M. *Hemoglobin and Myoglobin in their Reactions with Ligands*; Elsevier: Amsterdam, 1971.

(3) Dickerson, R. E.; Geis, I. *Hemoglobin: Structure, Function, Evolution and Pathology*; Benjamin-Cummings: Menlo Park, CA, 1983.

(4) Perutz, M. F.; Fermi, G.; Luisi, B.; Shaanan, B.; Liddington, R. C. *Acc. Chem. Res.* **1987**, *20*, 309−321.

(5) Perutz, M. *Mechanisms of Cooperativity and Allosteric Regulation in Proteins*; Cambridge University Press: Cambridge, England, 1990.

(6) Perutz, M. F.; Wilkinson, A. J.; Paoli, M.; Dodson, G. G. *Annu. Rev. Biophys.* **1998**, *27*, 1−34.

(7) Bashford, D.; Chothia, C.; Lesk, A. M. *J. Mol. Biol.* **1987**, *196*, 199−216.

(8) Sharma, V. S.; John, M. E.; Waterman, M. R. *J. Biol. Chem.* **1982**, *257*, 11887−11892.

(9) Shaanan, R. *J. Mol. Biol.* **1983**, *171*, 31−59.

(10) Springer, B. A.; Sligar, S. G.; Olson, J. S.; Phillips, G. N., Jr. *Chem. Rev.* **1994**, *94*, 699−714.

(11) Collman, J. P.; Brauman, J. I.; Halbert, T. R.; Suslick, K. S. *Proc. Natl. Acad. Sci., U.S.A.* **1976**, *73*, 3333−3337.

(12) Marks, G. S.; Brien, J. F.; Nakatsu, K.; McLaughlin, B. E. *Trends Pharmacol. Sci.* **1991**, *12*, 185−188.

10.1021/ja004168w CCC: $20.00 
Published on Web 04/17/2001

ideal disposition of His E7 relative to that in the ligand, and the fact that mutation of His E7 influences the $O_2$ affinity much less in the $\beta$- than in the $\alpha$-subunit.[13] Another role attributed to the distal His involves steric destabilization of Fe−CO bonding by distorting the ligand from the preferred heme normal,[11,14] although mutagenesis studies suggest that this effect is much less important than the hydrogen bonding role.[10,13] On the other hand, the reduced affinity of T-state Hb has been proposed to result from tension in the axial iron−His F8 bond that impedes the movement of the iron into the heme plane that is necessary for effective $O_2$ binding.[5,6] While the T-quaternary structure is referred to as tense, this axial tension really does not significantly manifest itself in the deoxy Hb form because the iron is expected to be well out of the heme plane, as found in models. It is primarily upon ligation that the tension is developed, and this has been convincingly demonstrated recently for Hb with the link between the F helix and imidazole severed by mutagenesis,[15] and in the cyanide-ligated metHb located in a T-quaternary state in a single crystal, where in fact, the iron−HisF8 bond is ruptured in the $\alpha$-subunit.[16]

The detection of "tension", without rupture, in an axial bond crystallographically is problematical since the bond length changes can be much less than the available resolution. In principle, solution spectroscopy offers an alternate route to monitoring bond strain in the proximal His. Two such spectroscopies are resonance Raman (RR),[17] which detects the Fe−His bond through its stretching frequency, and $^1$H NMR of paramagnetic Hb,[18−21] which detects the Fe−His bond via spin density delocalized from the iron to the imidazole ring. In practice, these methods depend on the detection and firm assignment of the spectra, which has largely limited both studies to the high-spin ferrous or deoxy Mb, Hb, for which both detect, albeit small, Fe−His bond weakening on the R → T conversion.[17,18] The cyanomet derivatives of Mb and Hb can serve as a model for both CO and $O_2$ binding, since, like $O_2$, it is a (weaker) hydrogen bond acceptor[22] and, like CO, would experience steric tilting by interaction with distal residues.[23−25] Moreover, oxidation/ligation state valency hybrids with cyanomet $\alpha$- or $\beta$-subunits,[26,27] as well as certain mutant Hbs,[28] can be induced to undergo the R → T quaternary transition upon binding organic phosphate, protons or ligation on the ferrous $\beta$- or $\alpha$-subunit, respectively. The key proximal and distal His signals in monomeric metMbCN have been assigned[29−31] and shown to be sensitive to the detailed molecular structure of the distal cavity.[20,21,32] Similar assignments of tetrameric metHbCN have not been reported because of the severe broadening and increased spectral congestion due to the subunit heterogeneity and large size (∼65 kDa) of HbA. The paramagnetic cyanomet form, in addition to strongly facilitating the detection and assignment of the distal His labile protons,[25,29] provides a unique spectroscopic signature for the heme that reflects the presence or absence of a distal hydrogen bond to the cyanide. Thus, elimination of the hydrogen bond to the ligated $CN^-$ in models[33] and metMbCN complexes[34] or resting state, cyanide-ligated heme peroxidase[35] leads to a ∼1 ppm decrease in the mean methyl shift for the heme.

1D/2D NMR appropriately tailored[36,37] to the paramagnetism and size, together with judicious use of the temperature dependence of hyperfine shifts,[38] has allowed the complete assignment of the heme and a large portion of the active-site protons >6 Å from the iron for metHbCN.[25] The spectral congestion, however, left the key axial His F8 ring protons undetected and the key distal His ring protons, in particular the labile proton involved in the hydrogen bond to the ligand, unassigned.[25] We present herein the results of a detailed $^1$H NMR study of the proximal and distal His in metHbCN to unambiguously assign both residues in each of the two subunits, assess the nature of the Fe−His covalency by determination of the His F8 ring shifts for comparison with similar data on "relaxed" metMbCN,[23,31] gauge whether the orientation of the $\alpha$-subunit distal His is closer to that found in the HbCO or $HbO_2$ crystal structure,[9,39] and determine the nature of any hydrogen bond between the distal His ring and the bound $CN^-$ in each subunit. To facilitate the assignment process in the tetramer, as well as to gain some insight into the effect of tetramer assembly on the roles of the two His, we initiate the assignments on the cyanomet forms of the isolated chains of HbA.[40]

## Experimental Section

**Proteins.** HbA was isolated and purified, and the cyanomet complex of HbA and methbCN and the cyanomet complexes of the isolated $\alpha$- and $\beta$-chains, met-$\alpha$-CN and met-$\beta$-CN, were prepared by standard procedures[2,41] as described in detail previously.[42] Prior to NMR measurements, the cyanomet globin complexes were buffer-exchanged and concentrated in an Amicon ultrafiltration cell to a final concentration ∼2 mM in 50 mM phosphate buffer, 20 mM NaCl, 40 mM KCN, pH 5.4 or 8.4; 10% $^2H_2O$ was added to the $^1H_2O$ solutions for the spectrometer lock. The purity of each sample was established on the

(13) Mathews, A. J.; Rohlfs, R. J.; Olson, J. S.; Tame, J.; Renaud, J.-P.; Nagai, K. *J. Biol. Chem.* **1989**, *264*, 16573−16583.
(14) Kuriyan, J.; Wilz, S.; Karplus, M.; Petsko, G. A. *J. Mol. Biol.* **1986**, *192*, 133−154.
(15) Barrick, D.; Ho, N. T.; Simplaceanu, V.; Dahlquist, F. W.; Ho, C. *Nat. Struct. Biol.* **1997**, *4*, 78−83.
(16) Paoli, M.; Dodson, G.; Liddington, R. C.; Wilkinson, A. J. *J. Mol. Biol.* **1997**, *271*, 161−167.
(17) Spiro, T. G. *Resonance Raman Spectroscopy of Hemes and Hemoproteins*; Wiley-Interscience: New York, 1988.
(18) Ho, C. *Adv. Protein Chem.* **1992**, *43*, 153−312.
(19) Ho, C.; Perussi, J. R. *Methods Enzymol.* **1994**, *232*, 97−138.
(20) Bertini, I.; Turano, P.; Vila, A. J. *Chem. Rev.* **1993**, *93*, 2833−2932.
(21) La Mar, G. N.; Satterlee, J. D.; de Ropp, J. S. In *The Porphyrins Handbook*; Kadish, K. M., Guilard, R., Smith, K. M., Eds.; Academic Press: San Diego, 1999; Vol. 5, pp 185−298.
(22) Lecomte, J. T. J.; La Mar, G. N. *J. Am. Chem. Soc.* **1987**, *109*, 7219−7220.
(23) Emerson, S. D.; La Mar, G. N. *Biochemistry* **1990**, *29*, 1556−1566.
(24) Rajarathnam, K.; Qin, J.; La Mar, G. N.; Chiu, M. L.; Sligar, S. G. *Biochemistry* **1994**, *33*, 5493−5501.
(25) Kolczak, U.; Han, C.; Sylvia, L. A.; La Mar, G. N. *J. Am. Chem. Soc.* **1997**, *119*, 12643−12654.
(26) Ogawa, S.; Shulman, R. G. *J. Mol. Biol.* **1972**, *70*, 315−336.
(27) Mukerji, I.; Spiro, T. G. *Biochemistry* **1994**, *33*, 13132−13139.
(28) Kim, H.-W.; Shen, T.-J.; Sun, D. P.; Ho, N. T.; Madrid, M.; Ho, C. *J. Mol. Biol.* **1995**, *248*, 867−882.
(29) Lecomte, J. T. J.; La Mar, G. N. *Eur. Biophys. J.* **1986**, *13*, 373−381.
(30) Emerson, S. D.; La Mar, G. N. *Biochemistry* **1990**, *29*, 1545−1555.
(31) Nguyen, B. D.; Xia, Z.; Yeh, D. C.; Vyas, K.; Deaguero, H.; La Mar, G. *J. Am. Chem. Soc.* **1999**, *121*, 208−217.
(32) Yamamoto, Y. *Ann. Rep. NMR Spectrosc.* **1998**, *30*, 1−77.
(33) La Mar, G. N.; Del Gaudio, J.; Frye, J. S. *Biochim. Biophys. Acta* **1977**, *498*, 422−435.
(34) Nguyen, B. D.; Xia, Z.; Cutruzzolá, F.; Travaglini Allocatelli, C.; Brancaccio, A.; Brunori, M.; La Mar, G. N. *J. Biol. Chem.* **2000**, *275*, 742−751.
(35) de Ropp, J. S.; Sham, S.; Asokan, A.; Newmyer, S. L.; Ortiz de Montellano, P. R.; La Mar, G. N. Manuscript in preparation.
(36) La Mar, G. N.; de Ropp, J. S. *Biol. Magn. Reson.* **1993**, *18*.
(37) Bertini, I.; Luchinat, C. *Coord. Chem. Rev.* **1996**, *150*, 1−296.
(38) Qin, J.; La Mar, G. N. *J. Biomol. NMR* **1992**, *2*, 597−618.
(39) Baldwin, J. *J. Mol. Biol.* **1980**, *136*, 103−128.
(40) Ogawa, S.; Shulman, R. G.; Yamane, T. *J. Mol. Biol.* **1972**, *70*, 291−300.
(41) Ikedo-Saito, M.; Inubishi, T.; Yonetani, T. *Methods Enzymol.* **1981**, *76*, 131−121.
(42) Yamamoto, Y.; La Mar, G. N. *Biochim. Biophys. Acta* **1989**, *996*, 187−194.

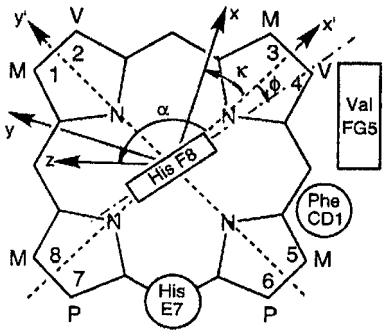


**Figure 1.** Dispositions of His F8 and Phe CD1, Val FG5, and His E7 relative to the heme in HbA. Also shown are the reference coordinate system, $x'$, $y'$, $z'$, with $z'$ normal to the heme plane, and the magnetic coordinate system, $x$, $y$, $z$, where $\beta$ (not shown) is the tilt of the $z$-axis from the heme normal, $\alpha$ defines the projection of the $z$-axis tilt on the heme plane and the $x'$-axis, and $\kappa \approx \alpha + \gamma$, locates the rhombic magnetic axes.

basis of comparison of the $^1$H NMR spectra with those reported previously for the cyanomet complexes of the tetramer[25] and isolated chains.[43]

**NMR Spectra.** All $^1$H NMR data were collected on a GE Ω500 spectrometer operating at 500 MHz. Normal reference spectra were collected over 20 kHz bandwidth with 4096 points at a repetition rate of 1 s$^{-1}$. WEFT spectra were recorded[44] to enhance detectability and characterization of strongly relaxed protons by suppressing weakly relaxed protons using a relaxation delay of 10−65 ms and repetition rates of 5−10 s$^{-1}$. Nonselective $T_1$'s were estimated (±15%) from the initial recovery of the magnetization in a standard inversion−recovery pulse sequence. When necessary, the solvent signal was saturated during the relaxation data. The distance to the iron for a proton $i$, $R_i$, was estimated from the relation[20,21,36,37]

$$R_i = R_r(T_{1i}/T_{1r})^{1/6} \quad (1)$$

where r is a reference proton (His F8 $N_\delta H$ $R = 5.0$ Å).

Steady-state NOEs were carried out as described in detail previously,[30,45] with the decoupler frequency in the reference spectrum placed symmetric to the peak of interest. When this was not possible, the validity of an NOE was established by observing NOEs that are proportional to degree of saturation as a function of decoupled power.[46] NOESY[47] (mixing time 35−45 ms) and clean-TOCSY[48] (mixing times 20−30 ms) spectra were recorded over a 20 kHz bandwidth using 2048 t2 points and 512 t1 blocks of 160 scans at recycle time of 2 to 3 s$^{-1}$. 1D spectra were apodized by 10 Hz linebroadening. 2D data sets were apodized by 30°-shifted sine-bell-squared in both dimensions, and zero-filled to 2048 × 2048 points prior to Fourier transformation.

**Magnetic Axes.** The orientation of the magnetic axes, ($\alpha$, $\kappa \approx \alpha + \gamma$ defined in Figure 1; $\beta$ tilt of $z$ from $z'$), was determined for each subunit by minimizing the global error function, $F/n$[23,49]

$$F/n = \sum^{n} |\delta_{dip}(obs) - \delta_{dip}(calc)|^2 \quad (2)$$

where the observed dipolar shift for nonligated residue protons, $\delta_{dip}$(obs) is given by:

$$\delta_{dip}(obs) = \delta_{DSS}(obs) - \delta_{DSS}(HbCO) \quad (3)$$

where $\delta_{DSS}$(obs) and $\delta_{DSS}$(HbCO) are the observed chemical shifts relative to 2,2-dimethyl-2-silapentane-5-sulfonate, DSS, in the paramagnetic metHbCN and diamagnetic HbCO complex,[50−52] respectively, as described in detail previously.[25] The calculated dipolar shift is given by:

$$\delta_{dip}(calc) = (12\pi N_A)^{-1}\Big[\Delta\chi_{ax}(3\cos^2\theta' - 1)R^{-3} + \frac{2}{3}\Delta\chi_{ax}(\sin^2\theta'\cos 2\Omega')R^{-3}\Big]\Gamma(\alpha,\beta,\gamma) \quad (4)$$

where $R$, $\theta'$, $\Omega'$ are the reference coordinates in an X-ray based, iron-centered coordinate system, $x'$, $y'$, $z'$, with $z'$ normal to the heme, as shown in Figure 1. $\Gamma(\alpha, \beta, \gamma)$ is the Euler rotation that rotates the reference coordinates into the magnetic coordinate, $x$, $y$, $z$, when the paramagnetic susceptibility tensor, $\chi$, is diagonal.[21,23,49] $\Delta\chi_{ax} = 2.48 \times 10^{-8}$ m$^3$/mol and $\Delta\chi_{rh} = -0.58 \times 10^{-8}$ m$^3$/mol are the axial and rhombic anisotropies that have been accurately determined for isoelectric metMbCN[31] and found to be invariant over a wide range of cyanomet Mb and Hb complexes.[24,34,53,54] The orientation of the magnetic axes are described by tilt $\beta$ of the major axis from the heme normal, in a direction defined by $\alpha$, the angle between the $z$ axis projection on the heme plane and the $x'$ axis, with the rhombic axes defined by $\kappa \approx \alpha + \gamma$, as shown in Figure 1. The necessary geometric factors in eq 4 were determined from the presumed isostructural HbCO[39] or $HbO_2$[9] crystal coordinates.[25] Input $\delta_{dip}$(obs) and $\delta_{dip}$(calc) were restricted to the proximal or F-helix[25,55] whose structure is essentially the same in the HbCO and $HbO_2$ crystals and is assumed conserved in metHbCN. The diamagnetic chemical shifts, $\delta_{DSS}$(dia), for the His E7 side chain with perturbed orientation were calculated using standard source of the peptide shifts[56] and effect of ring current[27,57] and secondary structure,[58] as described in detail elsewhere.[24,34,53,54,59]

## Results

**Heme Assignments in Isolated Chains.** The 500 MHz $^1$H NMR spectra of met-α-CN in $^1H_2O$ at acidic and alkaline pH are illustrated in Figures 2A and 3A, respectively, and those for met-$\beta$-CN are illustrated in Figure 4A,D, respectively and, except for the improved sensitivity and resolution, closely resemble those reported earlier.[40,43] The two low-field methyl peaks in each case had been assigned to 5-$CH_3$ and 1-$CH_3$ by isotope labeling.[43] TOCSY locates two three-spin (vinyls) and two four-spin (propionate) systems with significant hyperfine shifts which exhibit NOESY cross-peaks to two resolved methyl peaks and two partially resolved methyl peaks in the aromatic window that lead to the complete assignment of the pyrrole substituents in each of the isolated subunits in a manner as

(43) La Mar, G. N.; Jue, T.; Nagai, N.; Smith, K. M.; Yamamoto, Y.; Kauten, R. J.; Thanabal, V.; Langry, K. C.; Pandey, R. K.; Leung, H.-K. *Biochim. Biophys. Acta* **1988**, *952*, 131−141.
(44) Gupta, R. K. *J. Magn. Reson.* **1976**, *24*, 461−465.
(45) Thanabal, V.; de Ropp, J. S.; La Mar, G. N. *J. Am. Chem. Soc.* **1988**, *110*, 3027−3035.
(46) Lecomte, J. T. J.; Unger, S. W.; La Mar, G. N. *J. Magn. Reson.* **1991**, *94*, 112−122.
(47) Jeener, J.; Meier, B. H.; Bachmann, P.; Ernst, R. R. *J. Chem. Phys.* **1979**, *71*, 4546−4553.
(48) Griesinger, C.; Otting, G.; Wüthrich, K.; Ernst, R. R. *J. Am. Chem. Soc.* **1988**, *110*, 7870−7872.
(49) Williams, G.; Clayden, N. J.; Moore, G. R.; Williams, R. J. P. *J. Mol. Biol.* **1985**, *183*, 447−428.
(50) Craescu, C. T.; Mispelter, J. *Eur. J. Biochem.* **1989**, *181*, 81−96.
(51) Martineau, L.; Craescu, C. T. *Eur. J. Biochem.* **1992**, *205*, 661−670.
(52) Martineau, L.; Craescu, C. T. *Eur. J. Biochem.* **1993**, *214*, 383−393.
(53) Qin, J.; La Mar, G. N.; Cutruzzolá, F.; Travaglini Allocatelli, C.; Brancaccio, A.; Brunori, M. *Biophys. J.* **1993**, *65*, 2178−2190.
(54) Nguyen, B., D.; Zhao, X.; Vyas, K.; La Mar, G. N.; Lile, R. A.; Brucker, E. A.; Phillips, G. N., Jr.; Olson, J. S.; Wittenberg, J. B. *J. Biol. Chem.* **1998**, *273*, 9517−9526.
(55) The same 22 proximal side proton data were used as reported earlier. These protons include for the α/β subunit: Tyr/Phe C7 $C_\delta$Hs, $C_\epsilon$Hs; Phe CD1 $C_\zeta$H, $C_\epsilon$Hs, $C_\delta$Hs; Val E11 $C_a$H; Ala E14 $C_a$H, $C_\beta H_3$; Leu F4 $C_\alpha$H; Ser F5 $C_\alpha$H, $C_\beta$H; Asp/Glu F6 $C_\alpha$H; Leu F7 $C_\alpha$H, $C_{\beta1}$H, $C_{\beta2}$H; Ala/Cys F9 $C_\alpha$H; Val FG5 $C_\alpha$H, $C_\beta$H, $C_{\gamma1}H_3$, $C_{\gamma2}H_3$; Phe G5 $C_\delta$Hs, $C_\epsilon$Hs.
(56) Bundi, A.; Wüthrich, K. *Biopolymers* **1979**, *18*, 285−297.
(57) Cross, K. J.; Wright, P. E. *J. Magn. Reson.* **1985**, *64*, 240−231.
(58) Wishart, D. S.; Sykes, B. D.; Richards, F. M. *J. Mol. Biol.* **1991**, *222*, 311−333.
(59) Rajarathnam, K.; Qin, J.; La Mar, G. N.; Chiu, M. L.; Sligar, S. G. *Biochemistry* **1993**, *32*, 5670−5680.

**Table 1.** Chemical Shifts for the Heme Methyls, Proximal His F8, and Distal His E7 and Phe CD1 in the Cyanomet Derivatives of the Isolated Chains and the Intact Tetramer of Human HbA at pH 8.4 and 30° C[a]

| residue | proton | symbol[b] | isolated α-chain | intact tetramer α-subunit | intact tetramer β-subunit | isolated β-chain |
|---|---|---|---|---|---|---|
| Heme | 1-$CH_3$ | $M_1$ | 16.15 | 16.38[c] | 14.98 | 15.30 |
| | 3-$CH_3$ | | 8.17 | 8.04[c] | 8.04 | 8.83 |
| | 5-$CH_3$ | $M_5$ | 21.83 | 21.15[c] | 21.23 | 20.64 |
| | 8-$CH_3$ | | 8.75 | 8.37[c] | 8.67 | 8.93 |
| | $CH_3$[c] | | 13.73 | 13.49 | 13.23 | 13.43 |
| His F8 | NH | *c* | 13.18 | 13.48[c] | 13.16 | 13.24 |
| | $C_\alpha H$ | | 7.87 | 7.89[c] | 7.48 | 7.64 |
| | $C_\beta H$ | d | 9.90 | 10.23[c] | 10.16 | 9.59 |
| | $C_\beta H'$ | e | 6.66 | 6.82[c] | 7.18 | 6.50 |
| | $C_\delta H$ | f | −3.0 | −2.0 | −2.0 | −5.3 |
| | $C_\epsilon H$ | b | 18.0 | 17.4 | 17.4 | 20.4 |
| | $N_\delta H$ | *a* | 21.29 | 21.33[c] | 21.53 | 21.79 |
| His E7 | $N_\epsilon H$ | *i* | 16.29 | 16.41 | *d* | *d* |
| | $C_\delta H$ | j | 12.79 | 13.12[c] | 15.45 | 14.71 |
| | $C_\epsilon H$ | k | 0.19 | 0.52 | 2.11 | 0.41 |
| Phe CD1 | $C_\zeta H$ | g | 14.02 | 14.67[c] | 13.65 | 14.37 |
| | $C_\epsilon Hs$ | h | 8.83 | 8.97[c] | 8.83 | 9.36 |
| | $C_\delta Hs$ | | 6.68 | 6.64[c] | 6.93 | 7.03 |

[a] Chemical shift, in ppm from DSS, in $^1H_2O$ solution. [b] Symbols used in Figures 2−7. [c] The mean of the four heme methyl $\delta_{DSS}$(obs). [d] Not detected.

described in detail previously for both metMbCN[30,38] and the tetramer metHbCN (not shown).[25] The chemical shifts for the four methyl groups in the isolated chains, are listed in Table 1, where they are compared to the previously reported data on the tetramer.[25]

**Heme Pocket Assignment in the α-Chain.** Signals for amino acid residues in the dimeric α-chain are labeled by lower-case letter, with italic letters indicating labile protons. Two resolved labile protons (labeled *a* and *c*) are observed in Figure 2A at pH 5.4, one of which exhibits strong relaxation ($T_1(a) \approx 35$ ms) and the other is part of a TOCSY detected, hyperfine-shifted $NHC_\alpha HC_\beta H_2$ fragment (not shown). Peaks *a* and *c* exhibit a NOESY cross-peak between them and to the $C_\beta$Hs peaks (d, e) that are diagnostic of the proximal His F8 ring $N_\delta H$ (peak *a*) and the residue backbone NH (peak *c*) (data not shown), as found in intact metHbCN.[25] A WEFT-spectrum[44] designed to enhance broad, strongly relaxed resonances at the expense of narrow, weakly relaxed protons, reveals the presence of two very broad (∼500 Hz) and strongly relaxed ($T_1 \approx 3$ ms) peaks labeled b and f, as shown in Figure 2B; their retention in $^2H_2O$, together with the characteristic relaxation and line width, identify them as the two His F8 ring nonlabile protons.[30] Saturation of the low-field broad peak b in Figure 2C results in a significant NOE to the assigned His F8 $N_\delta H$ peak *a*, unambiguously assigning b to the His F8 $C_\epsilon H$, and indirectly, the upfield broad peak f to the $C_\delta H$. This assigns the complete His F8. NOESY cross-peaks between the heme 5-$CH_3$ and a TOCSY-detected, hyperfine-shifted three-spin system with Curie intercepts in the aromatic spectral window[30,60] and a resolved, strongly relaxed single proton peak g ($T_1 \approx 20$ ms), identifies the completely conserved distal Phe CD1 with g as the $C_\zeta H$ and h as the $C_\epsilon Hs$ signals (data not shown). The upfield methyl composite ($M_{FG5}s$) is part of a TOCSY-detected, relaxed Val with contact to 5-$CH_3$, as expected for Val FG5 and observed in the intact tetramer.[25]

When the $^1H$ NMR spectrum is recorded at pH 8.4, an additional, strongly relaxed proton peak labeled *i* is detected on the low-field side of the 1-$CH_3$ signal, as shown in Figure 3A, which *is absent at low pH*. The strong relaxation ($T_1 \approx$ 10−15 ms) of peak *i* is more evident in the WEFT-spectrum at pH 8.4, as shown in Figure 3B. The strong relaxation and large low-field shift is diagnostic of the $N_\epsilon H$ of the distal His ring in cyanide-ligated ferric globins[21,22] and peroxidases.[45] Saturation of this relaxed peak *i* in Figure 3C leads to comparable intensity NOEs to resolved and moderately relaxed ($T_1 \approx 45$ ms), nonlabile protons labeled j, and to an unresolved proton at 1.8 ppm labeled k. These shifts are both strongly temperature-dependent and must arise from the His E7 ring $C_\delta H$ and $C_\epsilon H$, respectively.[31,45] The His E7 $N_\epsilon H$ peak *i* also yields the expected weaker NOEs to peak h, the $C_\epsilon Hs$ of Phe CD1, and to the $6H_\beta s$, as shown in Figure 3C. A NOESY slice through the resolved peak j displays the expected NOEs for His E7 $C_\delta H$ to Phe CD1 $C_\epsilon Hs$ (h) and the $6H_\beta s$ (Figure 3D). Last, the NOESY slice through the resolved $6H_\beta$ exhibits, in addition to the expected NOEs to the other $6H_\beta$, $6H_\alpha s$, and 5-$CH_3$, a strong NOE to peak k, the His E7 $C_\epsilon H$, as well as to the $C_\epsilon H$ (peak h) of Phe CD1 (Figure 3E). Both the hyperfine shift pattern and relaxation properties, as well as the NOESY contacts, are diagnostic for the distal His E7 side chain, with *i*, j, and k peaks assigned to the $N_\epsilon H$, $C_\delta H$, and $C_\epsilon H$, respectively, of the ring in a fashion that is essentially identical to that observed in metMbCN.[30,31] The ring labile proton is clearly on the His E7 $N_\epsilon$ position in this subunit, as confirmed by its short $T_1 \approx 10-15$ ms. Lowering

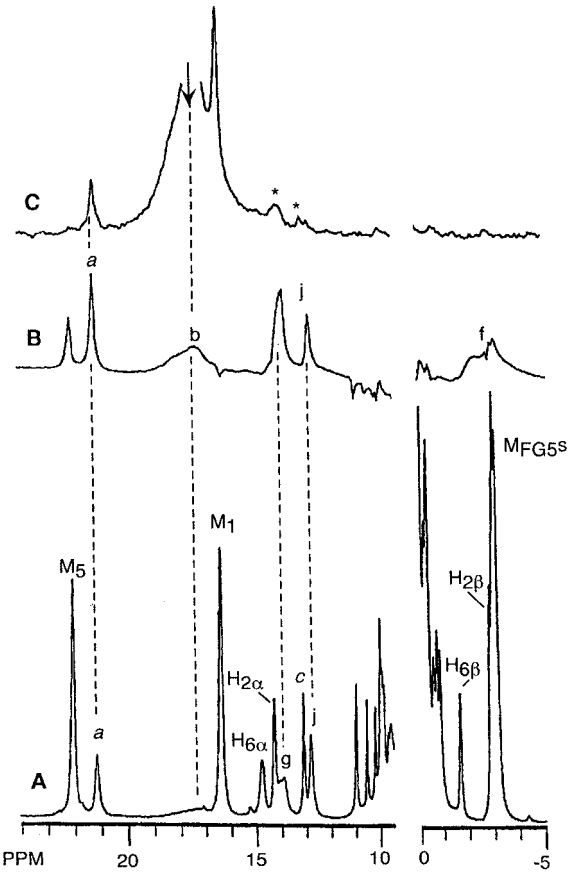


**Figure 2.** Resolved portions of the 500 MHz $^1H$ NMR spectra of the cyanomet form of the α-chain, met-α-CN, in $^1H_2O$, 50 mM phosphate, 100 mM NaCl, 40 mM KCN at 30 °C and pH 5.4: (A) reference spectrum collected under nonsaturating conditions; (B) WEFT spectrum (recycle time 200 ms, relaxation delay 60 ms) which emphasizes two broad and relaxed ($T_1 \approx 3$ ms) resonances in the low-field and upfield portions; (C) steady-state NOE difference spectrum upon partially saturating the broad, low-field peak b (marked by vertical arrow), with the decoupler of the reference trace placed symmetric to resonance *a* at 21.0 ppm.

(60) Emerson, S. D.; Lecomte, J. T. J.; La Mar, G. N. *J. Am. Chem. Soc.* **1988**, *110*, 4176−4182.

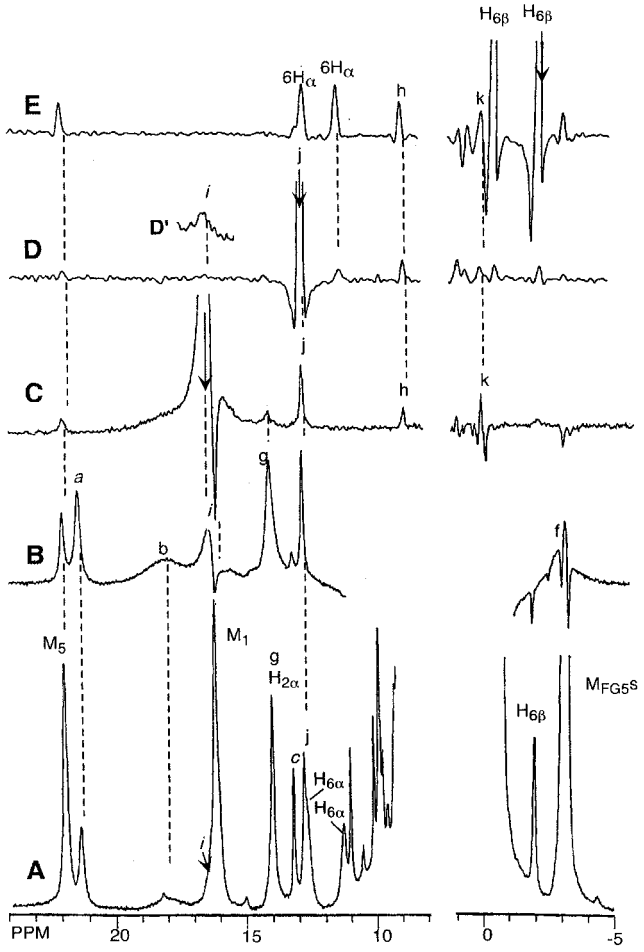


**Figure 3.** Resolved portions of the 500 MHz $^1$H NMR spectra of cyanomet form of the α-chain of HbA, met-α-CN, in $^1H_2O$, 50 mM phosphate, 100 mM NaCl, 40 mM KCN at 30 °C and pH 8.4: (A) reference spectrum recorded under nonsaturating conditions; (B) WEFT-spectrum (repetition time 200 ms; relaxation delay 60 ms) which emphasizes, in addition to the broad peaks detected in Figure 2B, a strongly relaxed, labile proton peak at 16 ppm labeled *i* (not observed in $^2H_2O$; not shown). (C) Steady-state NOE-difference spectrum upon saturating the labile proton peak *i*; (D) NOESY (35 ms mixing time; repetition time 333 ms) slice through the His E7 $C_\delta H$ and $6H_\alpha$ composite peak showing NOEs to $6H_\alpha$, $6H_\beta$s and Phe CD1 $C_\epsilon H$ (k), and $C_\delta H$ (j) peaks; (D′) shows weak NOE His E7 to $N_\epsilon H$ (peak *i*) upon saturating His E7 $C_\delta H$; (E) NOESY slice (35 ms mixing time; repetition time 333 ms) through $6H_\beta$ (shown by vertical arrow), showing, (in addition to cross-peaks to 5-$CH_3$ and the whole 6-propionate), the expected cross-peaks to the His E7 $C_\epsilon H$ peak k.

the pH of the sample leads to loss of intensity of the assigned His E7 $N_\epsilon H$ peak (not shown), with half intensity retained at pH 6.9, indicating saturation-transfer[61] from the solvent due to chemical exchange at acidic pH.

**Heme Pocket Assignments in the Isolated *β*-Chain.** Heme pocket residue signals for the tetrameric *β*-chain $^1$H NMR spectrum in Figure 4 are labeled by lower-case letters with an asterisk, with italics indicating labile protons. Two labile proton peaks, labeled *a** and *c**, are resolved with the former strongly relaxed ($T_1 \approx 35$ ms) and with TOCSY and NOESY connectivities identical to those of the $N_\delta H$ and $NpHC_\alpha HC_\beta H_2$ of His F8 as reported previously for metMbCN[30] and metHbCN,[25] and as found for met-α-CN above. WEFT-spectra in $^1H_2O$ at both low (Figure 4B) and high pH (Figure 4E) reveal the two broad (~1 kHz), strongly relaxed ($T_1 \approx$ 3ms), nonlabile

(61) Lecomte, J.; La Mar, G. N. *Biochemistry* **1985**, *24*, 7388−7395.

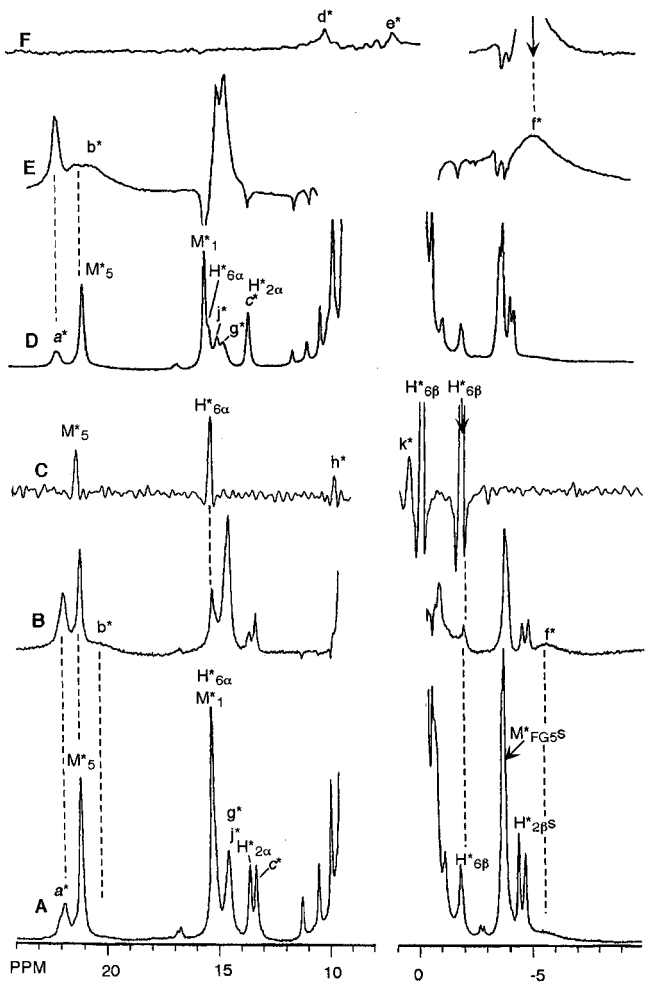


**Figure 4.** Resolved portions of the 500 MHz $^1$H NMR spectrum for the cyanomet derivative of the isolated *β*-chain of HbA, met-*β*-CN, in $^1H_2O$, 50 mM phosphate, 100 mM NaCl, 40 mM KCN at 30 °C and pH 5.4: (A) reference spectrum collected under nonsaturating conditions; and (B) WEFT-spectrum (repetition time 200 ms; relaxation delay 60 ms) that emphasizes the very broad and strongly relaxed ($T_1 \approx 3$ ms) protons in the low-field (b*) and high-field (f*) windows. (C) NOESY (40 ms mixing time; repetition time 333 ms) slice through $6H_\beta$ (shown by vertical arrow), with cross-peaks to 5-$CH_3$ and the complete 6-propionate, as well as to His E7 $C_\epsilon H$ peak k*. Resolved portions of the 500 MHz $^1$H NMR spectrum of the cyanomet complex of the isolated *β*-chain of HbA, met-*β*-CN, in $^1H_2O$, 50 mM phosphate, 100 mM NaCl, 40 mM KCN, at 30 °C and pH 8.4; (D) reference spectrum collected under nonsaturating conditions; (E) WEFT spectrum (repetition time 200 ms, relaxation delay 60 ms) that emphasizes strongly relaxed resonances b* and f*; (F) steady-state NOE-difference spectrum upon partially saturating the broad, upfield peak f* (shown by vertical arrow); note NOEs to the His F8 $C_\beta H$, $C_{\beta'} H$ that uniquely identify peaks *c**, d*, and f* to the His F8 $C_\delta H$ signal.

proton signals, b* and f*, that must originate from the His F8 ring. The low-field peak b* in this chain partially overlaps peak *a**, the assigned $N_\delta H$ of His F8. However, saturating the upfield broad peak f* at high pH results in NOEs to the assigned His F8 $C_\beta$Hs (d* and e*) (Figure 4F), confirming the peak f* assignment as the His F8 ring $C_\delta H$, and therefore, the low-field peak b* to the $C_\epsilon H$.

An NOE from the 5-$CH_3$ to two of the protons of a TOCSY-detected ring, together with the characteristic relaxation ($T_1 \approx$ 20 ms), identify peak g* and h* as the $C_\zeta H$ and $C_\epsilon$Hs of Phe CD1 (not shown). A resolved, moderately relaxed ($T_1 \approx 50$ ms) single proton peak j* is observed in the low-field spectrum at pH 8.4 (Figure 4D) where the His E7 $C_\delta H$ has been shown to

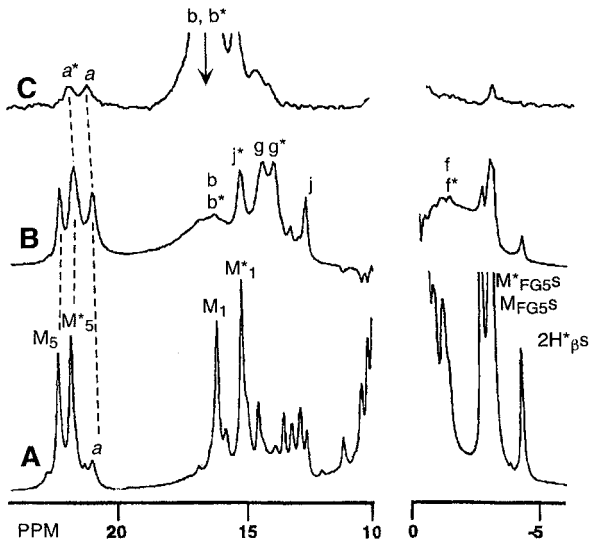


**Figure 5.** Resolved portions of the 500 MHz $^1$H NMR spectrum of metHbCN at 30 °C, 50 mM phosphate, 100 mM NaCl, 40 mM KCN, in $^1H_2O$ at pH 5.4: (A) reference spectrum collected under nonsaturating conditions; (B) WEFT spectrum (repetition time 200 ms, relaxation delay 60 ms) that emphasizes two very broad and strongly relaxed resonances labeled b, b* and f, f*. (C) steady-state NOE-difference trace upon partially saturating the broad low-field peak labeled b, b* (shown by vertical arrow); the assignment of the two detected NOEs to the His F8 $N_\delta H$ peaks *a* and *a** is shown in Figure 6.

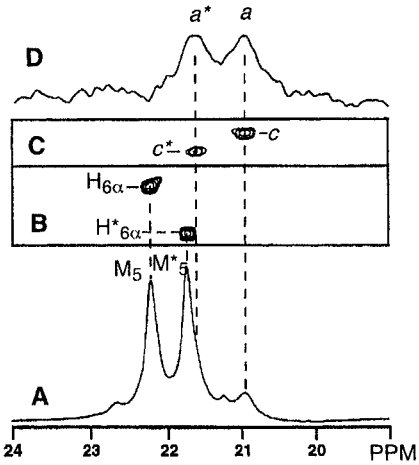


**Figure 6.** (A) Expanded portion of the low-field 500 MHz $^1$H NMR spectrum of metHbCN in $^1H_2O$, 50 mM phosphate, 100 mM NaCl, 40 mM KCN at 30 °C, pH 5.4 where the overlapping 5-$CH_3$ ($M_5$) and axial HisF8 $N_\delta H$ signals (*a*, *a**) for each of the two subunits resonate. Portions of the 45 ms mixing time NOESY spectrum that resolve the position of $M_5$, $M_5$*, *a* and *a** by the (B) $M_5$, $M_5$* to $H_{6\alpha}$, $H^*_{6\alpha}$ cross-peaks, and the (C) His F8 $N_\delta H$ (*a*) to $N_P H$ (*c*) and $N_\delta H$ (*a**) to $N_P H$ (*c**) cross-peak. (D) Steady-state NOE difference spectrum upon saturating the broad low-field peak b, b* (shown in Figure 5C). The two comparable intensity NOEs to *a* and *a** must arise from the simultaneous saturation of the degenerate HisF8 $C_\epsilon H$ peaks b and b* for the α and *β* subunits.

resonate in metMbCN,[30] metHbCN,[25] and in met-α-CN above. However, comparison of the spectra at low (Figure 4A,B) and high pH (Figures 4D, 4E) shows that there is no additional relaxed, low-field labile proton peak analogous to peak *i* observed at alkaline pH, as observed for met-α-CN above. In fact, no evidence for an additional low-field, relaxed labile proton peak could be obtained in the pH range 5.4−9.5 and temperature down to 5 °C. Peak j* is assigned to the His E7 $C_\delta H$ on the basis of its expected weak NOE to Phe CD1 (peak h*) at high pH (not shown). The other His E7 ring proton, peak k*, the $C_\epsilon H$, is assigned on the basis of its expected NOE from the 6-propionate $H_\beta$s, as shown in the NOESY slice in Figure 4C. Thus, it was not possible to obtain any direct evidence for a labile proton at position $N_\epsilon$ on the distal His. The *β*-chain assignments are summarized and compared to those of the *β*-subunit of the intact tetramer in Table 1.

**His F8 and His E7 Ring Assignments in HbA.** All weakly to moderately relaxed resolved resonances in metHbCN have been assigned to residues and individual subunit[25] by 2D NMR. Peaks for metHbCN in Figures 5−7 are initially labeled by lower-case letter (italics for labile protons) for the two subunits, with an asterisk identifying the *β* subunit. The backbone $NHC_\alpha$-$HC_\beta H_2$ fragments and ring $N_\delta H$ (peaks *a*, *a**) of His F8, the $C_\delta H$s (j, j*) of His E7, as well as the complete Phe CD1 (g, g* for $C_\zeta H$, h, h* for $C_\epsilon H$s) ring for each of the subunits in metHbCN have been assigned previously,[25] and the relevant data are compared to the data on the isolated chains in Table 1. Not located previously are the His F8 nonlabile ring protons or other protons on the His E7 ring. The normal $^1$H NMR spectrum of metHbA−CN at low pH is shown in Figure 5A. The WEFT spectrum in Figure 5B reveal two strongly relaxed ($T_1 \approx 3$ ms), comparably broad (∼1.5 kHz) and comparably intense peaks centered at 17 (b, b*) and −2 ppm (f, f*) that must originate from the His F8 ring protons[30] from either the α or *β*, or both subunits. Irradiation of the center of the low-field broad peak (labeled b, b*) leads to NOEs of *comparable intensities* for two peaks *a* and *a**, as shown in Figure 5C. Alignment of the two detected NOEs from saturating the peak at 17 ppm with the NOESY map that locates the previously reported[25] 5-$CH_3$ to $6H_\alpha$ and His F8 $N_P H$ (peak *a*, *a**) to His F8 $N_\delta H$ (peaks *c*, *c**) cross-peak in the subunit, as shown in Figure 6B,C, reveals that the identical magnitude NOEs from the 17 ppm peak arises from the His F8 $N_\delta H$s of the *two subunits*. Hence the peak b, b* at ∼17 must be a superposition of the $C_\epsilon H$s of the axial His *of both α(b) and β(b*) subunits*. Having established that the peak at 17 ppm arises from the degenerate His F8 $C_\epsilon H$s of the two subunits, the comparable intensity and line width of the upfield broad peak labeled f, f* in Figure 5B dictate that it arises from the essentially degenerate His F8 $C_\delta H$ peaks of the two subunits.

The conventional $^1$H NMR spectrum of metHbCN at alkaline pH suggests the presence of an additional relaxed, labile proton peak *i* under the α-subunit 1-$CH_3$ peak, $M_1$, in Figure 7A. The WEFT-spectrum in Figure 7B confirms the presence of such a peak at 16.3 ppm with an estimated $T_1(i) \approx 10-15$ ms; this peak is absent in $^2H_2O$ solution (not shown). Saturation of this labile proton peak *i* leads to comparably strong resolved NOEs to peak j and peak k at ∼0.5 ppm (see Figure 7C), of which peak j had been previously assigned His E7 $C_\delta H$ from *the α-subunit*[25] (as well as to the Phe CD1 $C_\epsilon H$ peak h). This assigns the labile proton peak *i* to the $N_\epsilon H$, and the 0.5 ppm peak k to the $C_\epsilon H$ of the α-subunit His E7. A NOESY slice through the resolved α-subunit $6H_\beta$ leads to the expected NOEs to the His E7 $C_\delta H$ (peak j) and $C_\epsilon H$ (k), as well as to the other $6H_\beta$, the $6H_\alpha$s and 5-$CH_3$ ($M_5$), as shown in Figure 7D. The intensity of the labile proton peak at 17 ppm is diminished at pH 7 and disappears below pH 6.5, indicating saturation-transfer from bulk water.[61]

The complete absence of NOEs to the *β*-subunit His E7 $C_\delta H$ upon saturating the labile proton peak *i* (Figure 7C) excludes the possibility that the distal His E7 labile proton peak for the *β*-subunit could be under that for the α-subunit. No evidence for an additional relaxed, low-field labile could be detected in the pH range 5.5−9.5 and down to 5 °C. The NOESY slice through the resolved *β*-subunit $6H_\beta$*, however, reveals the

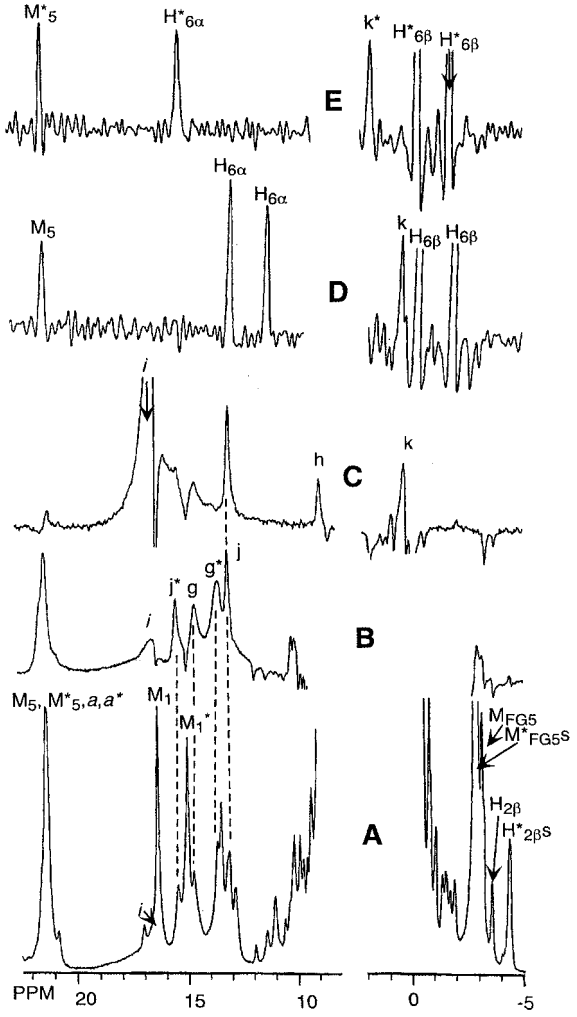


**Figure 7.** Resolved portions of the $^1$H NMR spectrum of metHbA−CN in $^1H_2O$, 50 mM phosphate, 100 mM in NaCl, 40 mM KCN, at 30 °C and pH 8.4; (A) reference spectrum collected under nonsaturating conditions; (B) WEFT-spectrum (repetition time 200 ms; relaxation delay 60 ms) that emphasizes broad peaks; note the appearance of a broad peak *i* at 16.2 ppm that is not present at low pH, (C) Steady-state NOE-difference spectrum upon saturating the strongly relaxed, low-field labile proton peak *i*; note NOEs to His E7 $C_\delta H$ peak j and Phe CD1 peak h of the α-subunit, as well as to His E7 $C_\epsilon H$ peak k; (D) NOESY slice (35 ms mixing time) through $6H_\beta$ (shown by vertical arrow) of α-subunit, with cross-peaks, in addition to 5-$CH_3$ and complete 6-propionate, to α-subunit His E7 $C_\delta H$ peak k and $C_\epsilon H$; (E) NOESY slice (35 ms mixing time) through $6H_\beta$* (shown by vertical arrow) of $\beta$-subunit, with cross-peaks, in addition to 5-$CH_3$ ($M^*_5$) and complete 6-propionate, to His E7 $C_\epsilon H$ peak k* of $\beta$-subunit.

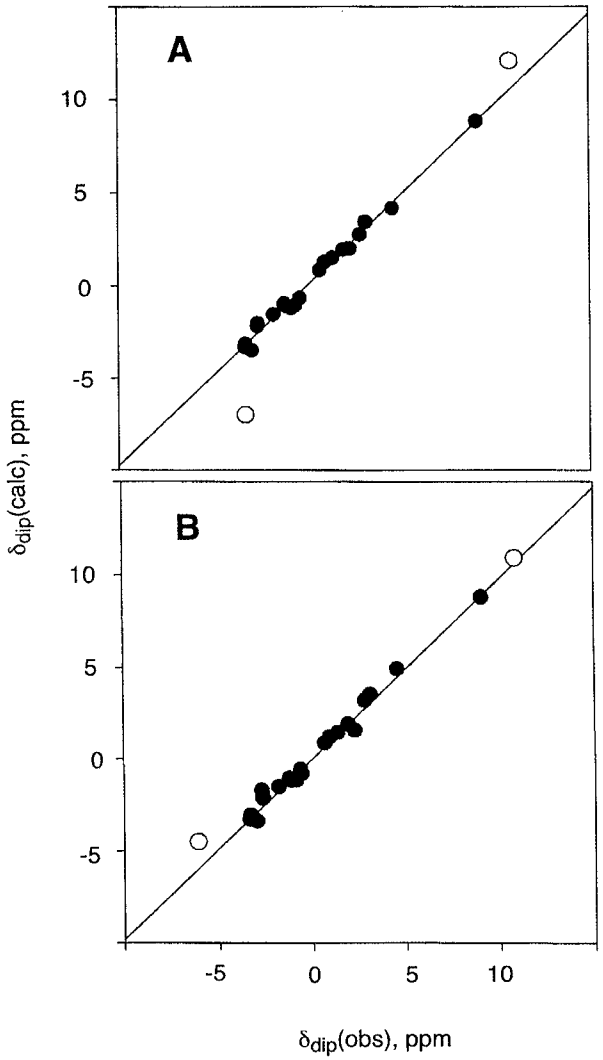


**Figure 8.** Plot of $\delta_{dip}$(obs) vs $\delta_{dip}$(calc) for the optimized magnetic axes for the $\beta$-subunit of metHbCN using the (A) $HbO_2$ crystal coordinates, and (B) the HbCO crystal coordinates. The points for the input data for the proximal helix are shown in closed circles. The values for the His E7 ring protons are shown as open circles for the orientations in the respective crystal structures. Note excellent correlation for the input data points and the generally good correlation for the HisE7 ring, indicating the residue has the same orientation as found in both HbCO and $HbO_2$.

expected NOEs to His E7 $C_\delta H$ (j*) and $C_\epsilon H$ (k*), as well as the other $6H_\beta$*, $6H_\alpha$*'s and 5-$CH_3$ ($M_5$*) (Figure 7E). The $^1$H NMR spectral properties of the His F8, His E7, and Phe CD1 protons in the isolated chains and the subunits for the intact tetramer are compared in Table 1.

**Magnetic Axes Determination and Modeling the His E7 Orientation.** The orientation of the magnetic axes for each subunit of metHbCN in alkaline pH have been reported[25] using the reported $\delta_{dip}$(obs) for the structurally conserved proximal helix,[55] $\Delta\chi_{ax} = 2.48 \times 10^{-8}$ m$^3$/mol, $\Delta\chi_{rh} = -0.58 \times 10^{-8}$ m$^3$/mol determined accurately from isoelectronic metMbCN,[31] and the crystal coordinates for either HbCO[39] or $HbO_2$.[9] The α, $\beta$, $\kappa$ values are 201°, 11°, 41° and 221°, 13°, 36° for the α-subunit using the HbCO[39] and $HbO_2$ coordinates,[9] respectively, and 170°, 10°, 32° and 171°, 10°, 48° for the $\beta$ subunit using the HbCO[39] and $HbO_2$ coordinates,[9] respectively. The high quality of the fits is emphasized in the plot of $\delta_{dip}$(obs) versus $\delta_{dip}$(calc) for the input data (closed circles) shown in Figure 8 for the $\beta$-, and in Figure 9 for the α-subunit of metHbCN. The magnetic axes for each subunit are within the uncertainties[31] for the determined values of $\beta$ (±1°), α (±10), and $\kappa$ (±10) for the HbCO and $HbO_2$ crystal coordinates, although they differ somewhat between the two subunits, as reported previously.[25] It is noted that, when $\delta_{dip}$(obs) and $\delta_{dip}$(calc) for the distal His E7 ring (open circles in Figures 8, 9) in their crystallographic orientation are compared, there is a large difference between the values obtained for His E7 orientation in the α-subunit (Figure 9), while the values are relatively well predicted for the $\beta$-subunit (Figure 8) for both HbCO and $HbO_2$. The position of the distal His E7 side chain relative to that of the heme in the $\beta$-subunit is very similar[9,39] in $HbO_2$ and HbCO, while that in the α-subunit intrudes much further into the pocket in the $HbO_2$ than HbCO form, as shown in Figure 10, which represents largely a change by ∼20−25° change in $\chi_1$ for His E7.

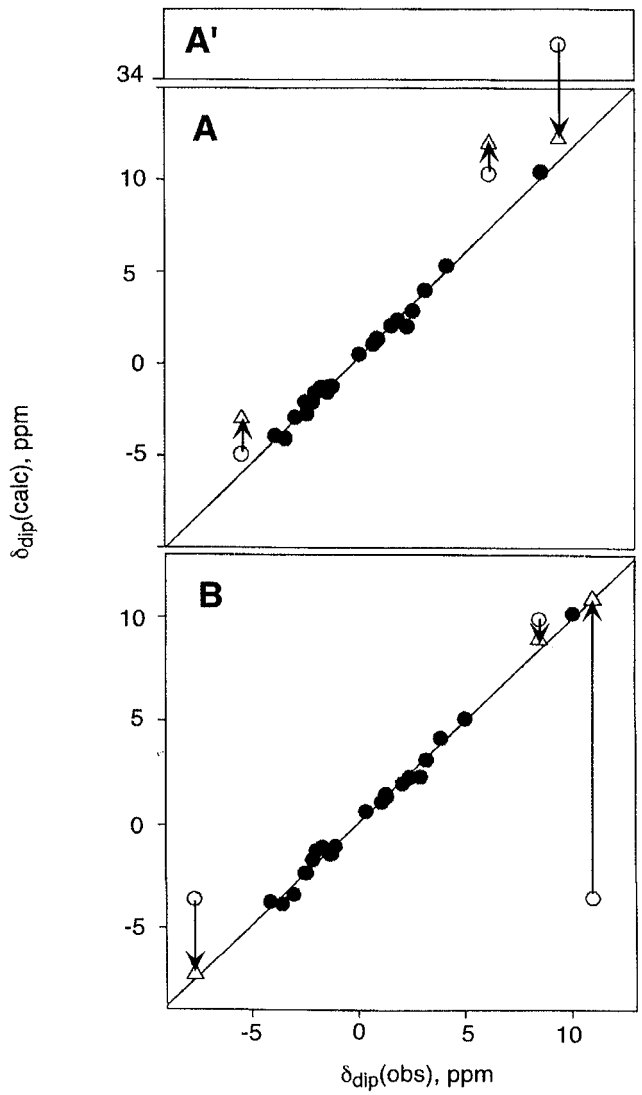


**Figure 9.** Plot of $\delta_{dip}$(obs) vs $\delta_{dip}$(calc) for the optimized magnetic axes for the α-subunit of metHbCN using the (A and A′) $HbO_2$ crystal coordinates; and (B) HbCO crystal coordinates. The points for the input data for the proximal helix are shown as closed circles.[55] The values for the His E7 ring protons are shown as open circles for the X-ray orientations of the residue. Note the excellent correlation for the input data points, but the large deviations, in opposite directions, for the His E7 side chain when using the HbCO or $HbO_2$ coordinates. The effect of changing by ∼12° in $HbO_2$, and by ∼10° in the opposite direction in HbCO results in very satisfactory correlation between the His E7 ring proton $\delta_{dip}$(obs) and $\delta_{dip}$(calc), as shown by open triangles.

The large discrepancies between $\delta_{dip}$(obs) and $\delta_{dip}$(calc) values for the α-subunit His E7 ring protons is concluded to arise from an orientation relative to the heme in metHbCN that is different from that found in either crystal structure, and is removed by either rotating the ring ∼10° further into the pocket than in HbCO,[39] or rotating by ∼12° further out of the pocket than in $HbO_2$,[9] as shown by the open triangles in Figure 9A,B, respectively. The ultimate α-subunit HisE7 orientation deduced for metHbCN starting with the alternate crystal structure is essentially the same and intermediate between the two as shown in Figure 10. It is noted that the fit starting with HbCO (Figure 9B) is better than that starting with $HbO_2$ (Figure 9A). Using the Phe CD1 $C_\zeta H$ ($T_1 \approx 20$ ms, $R_{Fe} \approx 4.4 \pm 0.2$ Å) as reference in eq 1, the α-subunit His E7 relaxation times for $C_\delta H$ ($T_1 \approx 45$ ms) and $N_\epsilon H$ ($T_1 \approx 10$ ms) lead to $R_{Fe}$ estimates of 5.2 ± 0.3 and 3.9 ± 0.2 Å, respectively. These are in reasonable agreement with the values for the same parameters in the optimized HisE7 orientation (5.5 and 3.6 ± 0.2 Å, respectively). The reported $T_1$ (HisE7 $C_\delta H$) ≈ 45 ms in the β-subunit of metHbCN is also consistent with the $R_{Fe} = 5.4 \pm 0.2$ Å found in the two crystal structures.

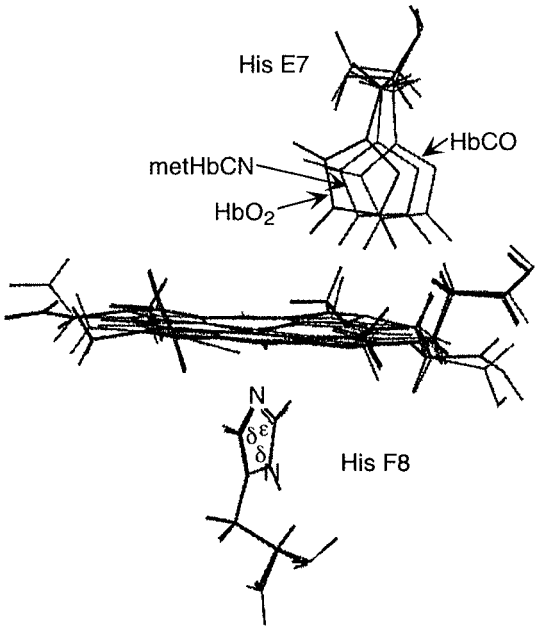


**Figure 10.** Superpositions of the heme and His F8 in the α-subunits of HbCO[39] and $HbO_2$,[9] showing the orientations of the His E7 within the heme pocket which differ largely in $\chi_1$ by ∼20−25°. The intermediate orientation of the His E7 ring is found in the α-subunit of metHbCN in solution.

## Discussion

**Orientation of His E7 in metHbCN.** The β-subunit HisE7 ring exhibits $\delta_{dip}$(obs) that are reasonably well predicted by either the HbCO or $HbO_2$ coordinates (Figure 8), which exhibit essentially the same His E7 side chain orientation.[9,39] The failure to detect the relaxed His E7 $N_\epsilon H$ signal precludes confirmation of the residue orientation using relaxation data. Hence we conclude that the β-chain His E7 has esssentially the same orientation for metHbCN in solution as in HbCO or $HbO_2$ crystals.[9,39] The α-subunit His E7 orientation differs significantly[9,39] in HbCO and $HbO_2$ as shown in Figure 10, and each predicts systematic deviations of $\delta_{dip}$ (calc) from $\delta_{dip}$(obs), but in opposite directions, as shown in Figure 9. Indeed, the optimized His E7 orientation is found intermediate between that in $HbO_2$ and HbCO, as illustrated in Figure 10. We conclude that the combination of the dipolar shift and relaxation constraints allows a reasonably robust determination of the distal His E7 orientation in metHbCN. It is furthermore anticipated that changes in the His E7 orientation due to point mutation should be similarly readily described by the dipolar shifts.

**Effect of Tetrameric Assembly.** The chemical shifts of both the heme methyls and the three strongly paramagnetically influenced residues, His F8, His E7, and Phe CD1 for a given globin chain are essentially the same in the isolated chain and subunit in the intact tetramer, as shown by the data in Table 1. Hence, we conclude that assembly of the R-state tetramer from the "relaxed", isolated subunits has only very minor influences on either the magnetic axes, as reflected in $\delta_{dip}$(obs) for noncoordinated residues such as Phe CD1 and His E7, or on the Fe−heme and Fe−His F8 bonding, as reflected in their conserved dominant contact shift values. Moreover, the His E7

$N_\epsilon H$ lability in the α-chain, as reflected in the loss of its intensity at acidic pH due to saturation transfer from bulk solvent,[61,62] is also inconsequentially altered upon assembly of the tetramer.

**Comparison between Cyanomet HbA and Mb.** The axial His F8 hyperfine shifts for each of the subunits of metHbCN (Table 1) are very similar to those reported for sperm whale metMbCN (with $C_\epsilon H$, $C_\delta H$ shifts of −4.6 and 18.3 ppm, respectively)[30] as is the orientation of the magnetic axes, which have been reported[31] with α, $\beta$, $\kappa$ values 190°, 15°, 38°, respectively. These comparisons support a "relaxed" or unstrained Fe−His F8 bond for both subunits of R-state metHbCN, as expected.[2−5,18,19] It is anticipated that the introduction of axial tension in the α-subunit by converting the R-state valency hybrid, (met-αCN)$_2$(deoxy-$\beta$)$_2$ to the T-state by binding inositol hexaphosphate,[26,27] should readily show up a characteristic effect on the axial His F8 ring hyperfine shifts and/or in changes in the orientation of the magnetic axes.

**Distal Hydrogen Bonding in the *β*-Subunit/Chain.** The distal His E7 in the α-subunit of metHbCN exhibits an $N_\epsilon H$ that is poised to provide a hydrogen bond to the bound cyanide, as in the crystal[9] of $HbO_2$. The His does not rotate into the heme pocket (when compared to HbCO) as far as in $HbO_2$ (see Figure 10), but this is likely due to the fact that Fe−O−O is highly bent, while the Fe−CN prefers to be linear, and is bent or tilted (as reflected in $\beta$ in the magnetic axes), and hence the His need not move as far as in $HbO_2$ to provide a hydrogen bond to the ligand.

The proton involved in this putative α-chain and α-subunit hydrogen bond is labile and exhibits an acid-catalyzed exchange rate that is very similar to that in sperm whale metMbCN,[61] where the proton was readily detected in alkaline pH but also exhibited progressive saturation-transfer from the solvent signal with decrease in pH until the peak was no longer detectable below pH 6. This behavior is very similar to the present observation on the α-subunit (or α-chain) His E7 $N_\epsilon H$ where the signal is similarly lost at pH 6. Thus, the strength of the hydrogen bonds between His E7 $N_\epsilon H$ and the bound cyanide are very similar in the Hb isolated α-chain, intact α-subunit, and sperm whale Mb. It is important to note that the absence of the His E7 $N_\epsilon H$ peak at lower pH in the α-chain/subunit *does not* indicate that the hydrogen bond is broken. Rather it indicates that the proton experiences limited protection from solvent by acid-catalyzed exchange, and this protection is a measure of the hydrogen bond strength.[61,62] For the same reason, the failure to detect the His E7 $N_\epsilon H$ labile proton in the $\beta$-subunit or $\beta$-chain even to pH 8.4 *does not* mean that the labile proton is not on $N_\epsilon$ or is not participating in a hydrogen bond with the cyanide. The evidence is equally consistent with the presence of such a hydrogen bond, but that it is somewhat weaker than in the α-subunit such that the lability is enhanced by a factor $\geq 10^2$ (and hence the dynamic stability decreased by $\geq 2.3$ kcal/mol[62]) when compared to that in the α-subunit.

Indirect evidence for the presence of a hydrogen bond between the $\beta$-subunit/chain His E7 $N_\epsilon H$ and the ligated cyanide can be drawn from the heme methyl contact shifts. It has been demonstrated in both model compounds[33] and cyanide-ligated ferric hemoproteins,[34,35,59,63] that abolishing the distal hydrogen bond to cyanide leads to a systematic ∼1 ppm *decrease* in the mean methyl hyperfine shift of the heme. This change in methyl shifts has been effected either by mutating the distal residue into a non-hydrogen bonding side chain,[59] or mutating residues that interfere with the ability of the distal His to orient itself into a position appropriate to forming a hydrogen bond to the bound cyanide.[34] Comparison of the heme mean methyl shift, $\delta_{DSS}(\overline{CH_3})$, for the two subunits in HbA, shown in Table 1, reveals that it is only marginally smaller (0.1 ppm) in the $\beta$- than α-subunit (chain). These results support the presence of a hydrogen bond between His E7 $N_\epsilon H$ and cyanide in the $\beta$- as well as α-subunit and chain, but with the hydrogen bond weaker in the former subunit or chain. It is of considerable interest and significance that recent $^1$H NMR data on isotope-labeled $HbO_2$ have, in fact, provided strong support[64] that, contrary to conclusions based on the $HbO_2$ crystal structure, the $\beta$-subunit HisE7 does indeed form a hydrogen bond to the bound $O_2$.

**Acknowledgment.** This research was supported by a grant from the National Institutes of Health, HL16087. The experimental assistance of Dr. J. S. de Ropp is gratefully acknowledged.

JA004168W

(62) Englander, S. W.; Kallenbach, N. R. *Q. Rev. Biophys.* **1984**, *16*, 521−655.

(63) Zhang, W.; Cutruzzolá, F.; Travaglini Allocatelli, C.; Brunori, M.; La Mar, G. N. *Biophys. J.* **1997**, *73*, 1019−1030.

(64) Lukin, J. A.; Simplaceanu, V.; Zou, M.; Ho, N. T.; Ho, C. *Proc. Natl. Acad. Sci. U.S.A.* **2000**, *97*, 10354−10358.